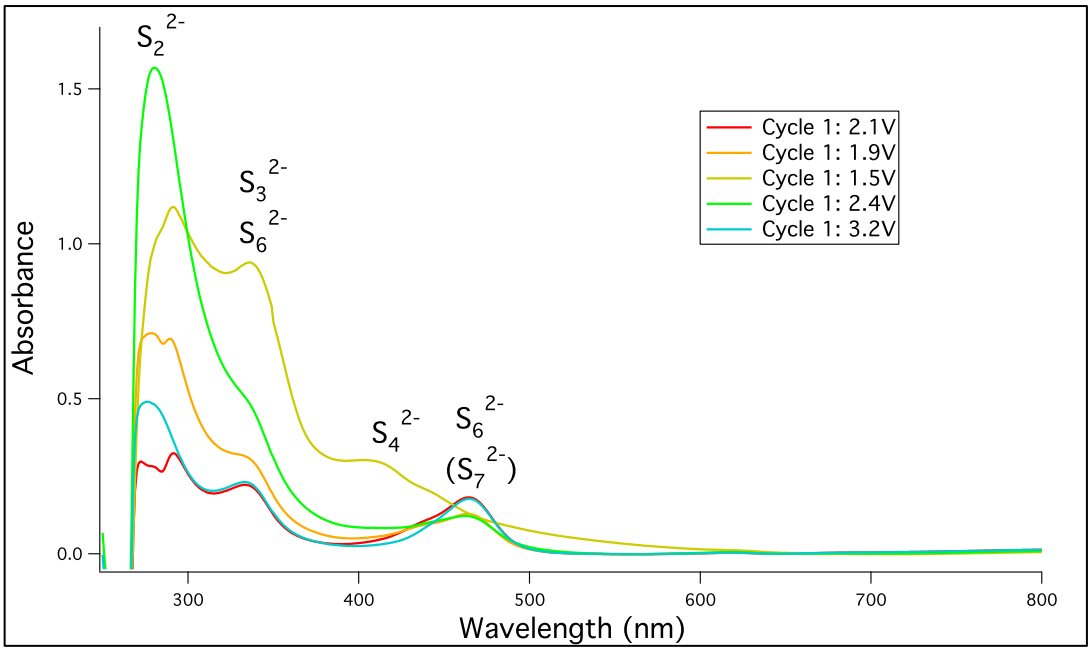
CHALMERS



Redox behavior of Li-S cell with PP14-TFSI ionic liquid electrolyte

Spectroscopic study on speciation of polysulfides during charge/discharge processes

Master of Science Thesis in the Master Degree Programme, Applied Physics

ERIK BLOMBERG

Department of Applied Physics
Division of Condensed Matter Physics
CHALMERS UNIVERSITY OF TECHNOLOGY
Gothenburg, Sweden, 2012

Thesis for the Degree of Master of Applied Physics

Redox behavior of Li-S cell with PP14-TFSI ionic liquid electrolyte

Spectroscopic study on speciation of polysulfides during charge/discharge processes

ERIK BLOMBERG

Department of Applied Physics
CHALMERS UNIVERSITY OF TECHNOLOGY
Göteborg, Sweden 2012

Redox behavior of Li-S cell with PP14-TFSI ionic liquid electrolyte
Spectroscopic study on speciation of polysulfides during charge/discharge processes
Erik Blomberg

Thesis for the Degree of Master of Applied Physics

© Erik Blomberg, 2012

Condensed Matter Physics
Department of Applied Physics
CHALMERS UNIVERSITY OF TECHNOLOGY
SE-412 96 Göteborg
Sweden www.chalmers.se Tel. +46-(0)31 772 1000

Cover: UV-Vis spectra indicating the polysufides present in the PP14-TFSI electrolyte of a Li-S cell during the first discharge and charge.
Printed by Chalmers Reproservice
Göteborg, Sweden 2012

Redox behavior of Li-S cell with PP14-TFSI ionic liquid electrolyte

Spectroscopic study on speciation of polysulfides during charge/discharge processes

Erik Blomberg
Department of Applied Physics, Chalmers University of Technology

Abstract

Li-S batteries, having one of highest theoretical energy densities possible, have been suggested as a way to improve on the current state of the art. However, the dissolution of intermediate polysulfide species in the electrolyte has so far greatly reduced the cycleabilty of these batteries. One proposed solution is to use an ionic liquid electrolyte to decrease the solubility of the polysulfides.

This work investigates the polysulfide speciation in Li-S cells with an ionic liquid electrolyte during charge and discharge. Four different room temperature ionic liquids were studied and found to dissolve polysulfides in small concentrations. One of the ionic liquids, PP14-TFSI, was examined further using UV-Vis spectroscopy to identify the polysulfide ions present in the electrolyte at different points of the charge/discharge cycle.

It was found that the first step of the reaction during discharge produces S_6^{2-} with only small amounts of other polysulfides. Most of the S_6^{2-} was then reduced to S_3^{2-} and S_4^{2-} in a second reaction step. These reactions showed good reversibility during charge, however a rapid decline in capacity was observed with continued cycling. This led to the conclusion that the ionic liquid did not by itself prevent the loss of active material associated with the dissolution of polysulfides.

Keywords: Lithium sulfur batteries, Li-S, ionic liquid electrolytes, polysulfides, UV-Vis spectroscopy.

Acknowledgements

This thesis would not have been possible without my supervisor Young Jin Choi, who never hesitated to answer the barrage of questions, give suggestions or show me how it's done. Thank you for your help and your support.
I would like to thank Aleksandar Matic for pushing me forward and, together with Per Jacobsson, providing excellent feedback and guidance. I also wish to thank the KMF group, some of you for being excellent office mates, others for keeping the labs and instruments running or enlisting my help in various projects, and all of you for creating a wonderful working environment.
Last but not least I thank my family and friends who I know I can rely on for love and support in all my endeavors.

Göteborg, June 2012
Erik Blomberg

Contents

Abstract i
Acknowledgements iii

1 Introduction **1**

2 Background **3**
2.1 The battery 4
2.1.1 Lithium-ion batteries 6
2.1.2 Lithium sulfur batteries 8
2.1.3 Ionic liquid electrolytes 10
2.2 Characterizing batteries 12

3 Materials & Procedures **14**
3.1 Ionic liquids 14
3.2 Reference sample preparation 15
3.3 UV-Vis spectroscopy 15
3.4 Cyclic Voltametry 17
3.5 Cell assembly and CV testing 18

4 Results & Discussion **21**
4.1 Reference samples 21
4.1.1 Raman spectroscopy 23
4.1.2 UV-Vis spectroscopy 24
4.2 Tested cells 27

5 Conclusion **32**

6 Future Work **33**

Bibliography **34**

List of Figures

2.1 The galvanic cell 3
2.2 The structure of PP14 11
2.3 The discharge curve 12

3.1 BRANDT™ UV cuvettes 16
(a) Cuvettes 16
(b) Absorption spectrum 16
3.2 The cyclic voltammogram 18
3.3 The Swagelok cell electrodes 19
3.4 The Swagelok cell 19

4.1 PP14-TFSI reference samples 21
4.2 PYR14-TFSI reference samples 22
4.3 BMIM-TFSI reference samples 22
4.4 BMIM-SCN reference samples 23
4.5 Raman spectra 24
4.6 PP14-TFSI UV-Vis spectra 24
4.7 Reference sample UV-Vis spectra 25
4.8 Peak intensity for the reference samples 26
4.9 Reference sample UV-Vis spectra after 28 d 27
4.10 A typical CV trace 28
4.11 UV-Vis spectra from cycle 1 29
4.12 UV-Vis spectra at 1.5 V 30
4.13 UV-Vis spectra at 3.2 V 31
4.14 UV-Vis spectrum from self-discharge test 31

Chapter 1

Introduction

Modern technology, and our use of it, is changing rapidly in many different and often unexpected ways. This evolution is often driven by advancements in key areas that enable a cascade of further improvements in various other fields. One good example is energy storage, which represent the second part of a problem as old as technology itself: how do we create the energy to power our machines and devices and how do we get it to the location and at the time where it is needed?

Efficient storage of electrical energy using rechargeable batteries, especially lithium ion (Li-ion) batteries, has proven to be the best solution for a range of applications. Their increasing use and rapid improvement have led to a multitude of dramatic changes, the most obvious being portable consumer electronics, and they are an important enabler for the development of electrified transportation and renewable energy distribution [1]. However, the desire for better performance (and lower cost) is driving todays batteries towards the theoretical energy density of the basic Li-ion chemistry. An increasing amount of R&D is therefore being directed towards alternative configurations and chemistries [1, 2]. One such candidate is to base the battery on the reaction between lithium and sulfur.

The specifics of the reaction between lithium and sulfur (Li-S) result in batteries with much higher specific energy than Li-ion batteries - in theory. The theoretical value for the specific energy, calculated using the capacity and voltages of the active materials, is a common way to compare different battery chemistries. The properties of elemental lithium and sulfur gives a specific energy of $2,567$ Wh/kg while the current Li-ion materials are limited to 387 Wh/kg [1]. In practice, that potential has been hard to realize because of multiple problems that degrade the performance and limit the life of the cells. The common approach to improve Li-S cells is the same as that which has been successfully applied to Li-ion:

changing the materials, especially the electrolyte, and the structure of the electrodes [1, 2, 3].

Ionic liquid electrolytes have been considered for use in batteries due to a number of beneficial properties, such as good ion conductivity, high electrochemical and thermal stability and low vapor pressure [4, 5, 6]. However, the specific application to Li-S batteries has only been studied quite recently [5, 7]. The aim of this thesis is to find another small piece of the puzzle by investigating the dissolution, transport and reactions of lithium polysulfide species in ionic liquid (IL) based electrolytes during charge and discharge of Li-S cells.

Chapter 2

Background

A battery is a device that stores electrochemical energy. The fundamental principles behind are the chemical reduction and oxidation (redox) reactions between two compounds. Such reactions occurs when the molecules or atoms of the two reactants exchange electrons in order to equilibrate their electrochemical potential μ, the energy released usually being in the form of heat and/or light. Greater control can be obtained by keeping the reactants separated and instead connecting them indirectly, resulting in an electrochemical reaction which can generate electrical currents and voltages in an external circuit. This also makes it possible to use an external power source to drive the reaction away from the spontaneous equilibrium.

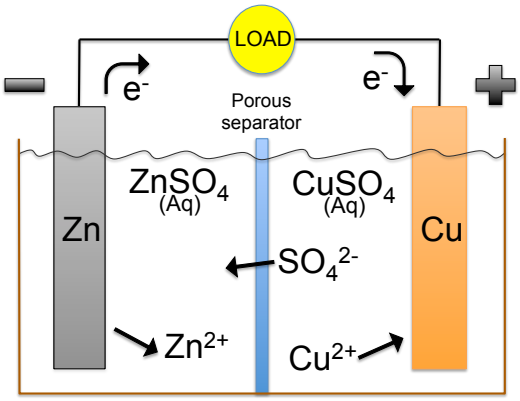


Figure 2.1: An example of a galvanic cell with one zinc and one copper electrode during discharge. The electrodes are immersed in separate aqueous electrolytes that are in ionic contact through a separator.

The galvanic cell, an example of which is shown in figure 2.1, is the most

common such arrangement. It consists of two electrodes containing the active materials that are in ionic, but not electric, contact through an electrolyte. The chemical reaction is thus split into two half reactions between each electrode and the electrolyte. These will proceed until they are suppressed by the increasing potential difference between the electrode and the electrolyte. When the electrodes are connected through an external electrical circuit a current will flow in order to neutralize the potential. This allows the reactions to continue, with an ionic current in the electrolyte and a corresponding external electric current, until all of the active material has been consumed. The energy released by the chemical reaction, ΔG, is given by

$$\Delta G = -nFE \tag{2.1}$$

and is in this arrangement mostly in the form of useful electrical power in the connected load. The energy is related to the number of electrons exchanged, n (per mol reactants), and $E = \Delta\mu$, the difference in the electrochemical potential of the reactants [8]. F, Faradays constant, is simply the molar charge of the electron ($\approx$ 96485 C mol^{-1}). This relationship is obtained by examining the thermodynamics of a reversible chemical reaction, i.e. that it strives to minimize Gibbs free energy G.

Each half reaction can be analyzed separately with different values of E as compared to a common reference material. This is usually the Standard Hydrogen Electrode (SHE), measured at 25 °C and 1 atm in a 1 M solution, which results in the Standard Electrode Potential E° [9]. The total electromotive force (emf, the potential due to the charge separation) of the cell is then simply the difference between the values for the active materials. An element with a high (more positive) E° is readily reduced and therefore an oxidizer and an element with a lower (more negative) value is correspondingly easily oxidized and a reducer. During the spontaneous reaction of the cell the electrode with the lowest electrode potential will be oxidized, releasing electrons into the external circuit, and this electrode is referred to as the negative electrode. The electrode with the more positive electrode potential will be reduced, accepting electrons, and is thus called the positive electrode. They are also often named the anode and the cathode which can lead to confusion as their roles are reversed during charging with the positive electrode, now technically an anode, supplying electrons and the negative electrode, acting as a cathode, accepting electrons.

2.1 The battery

The term battery is, although often used that way, not synonymous with an electrochemical cell. The battery is the actual device, consisting of one or multiple

connected cells, and includes packaging and structural materials and often safety features and control electronics. Modern batteries often use a separator, a thin porous membrane soaked in an electrolyte, or an electrolyte gelled with a polymer, in order to have only a minimal separation between the electrodes. This increases the current that can be drawn from the battery by enabling faster ion transport and also minimizes the amount of electrolyte needed. Metal current collectors and conductive additives to the active electrode materials such as carbon powder are often necessary since many of the active materials or their reaction products are poor electric conductors.

Batteries are typically divided into two main categories: Primary batteries are usually assembled in their charged state and are discarded (and hopefully recycled) after use. The first useful batteries were of this type and today they span a wide range of sizes, chemistries and applications. A widely recognized example of a primary battery are the common household 1.5 V "alkaline" batteries used to power flashlights, toys, clocks etc. They rely on the reaction between zinc and manganese oxide using an alkaline electrolyte and are easy to produce and use, safe and have the best performance for their price range, especially for applications requiring somewhat larger currents [9].

Secondary batteries use reactions and layouts that enable reversible operation, meaning that when the battery has been drained it can be recharged and used again. They are therefore commonly known as rechargeable batteries or sometimes, mostly for lead-acid batteries, accumulators. These batteries are called secondary since they store electrical energy supplied from some other energy source, returning it in a secondary operation (discharge). The different requirements means that primary and secondary batteries normally have different electrode combinations, although there are some that are used in both types such as rechargeable alkaline batteries. Tradeoffs in design and material utilization mean that the secondary versions have a higher cost and lower capacity.

There are a number of different parameters for evaluating the performance of batteries, some important ones being: the specific energy [Wh/kg] and energy density [Wh/L], the specific power [W/kg] and power density [W/L], efficiency, temperature range, useful lifetime and of course cost. In this case lifetime does not refer to capacity as in "battery life" but to durability: how long in both time and, for secondary batteries, number of charge/discharge cycles the battery can deliver useful performance. Related factors are the storage life and self-discharge rate - all batteries will leak some of their stored charge over time, but some versions used for special applications can deliver according to specifications after sitting on a shelf for decades [8]. When evaluating secondary batteries it is also important to consider the efficiency of the energy storage which for most batteries is around 70-80%, with the cheaper nickel-metal hydride and alkali variants being as low as 55-60% and the more expensive Li-ion getting as high as 95% [9].

The relative importance of the various characteristics depends heavily on the application - a cellphone or laptop battery would optimize the specific energy and energy density to make it as light and small as possible while grid energy storage using large scale batteries is likely to focus on low total cost as a function of unit cost and lifetime fare more than any weight or volume considerations. Electric vehicles fall in between these two extremes (with rather different priorities for a high end sports car compared to a delivery van) while also needing sufficient power to accelerate quickly and recover energy while braking [9].

While the theoretical performance of a cell or a battery can be calculated from the properties of the active materials such as capacity [Ah/kg], electrode potential, conductivity, molar mass and density the obtained values are mostly useful for comparison. The actual performance figures are usually much worse due to the compromises made to obtain a practical battery. One example is the practical energy storage, which usually is at most $1/3$ of the theoretical value [1] due to all the materials that do not store energy (casing, current collectors, separators, electrolyte and so on) and the fact that it is impossible to use all of the active material. For secondary batteries the depth of discharge (DOD) is never 100% and deep cycling usually leads to shorter lifetime. The voltage of the battery also shows important deviations from the ideal. The open circuit voltage (OCV), the potential between the electrodes when there is no current, is often quite close to the theoretical emf, but the voltage will drop as soon as there is a current drawn due to the internal resistance of the battery and polarization at the electrolyte-electrode interfaces. The resistance increases as the battery is discharged as a result of the increasing concentration of reaction products and the decreasing concentration of unreacted material leading to a sloping discharge curve instead of the ideal flat voltage.

2.1.1 Lithium-ion batteries

Equation (2.1) can be used as the starting point when analyzing the performance of a battery based on specific materials. It is easy to see that an increased difference in the electrode potential of the positive and negative electrode, i.e. a larger E, gives an increased energy storage. Maximum specific energy and energy density are therefore achieved using electrode materials with large (negative or positive) electrode potentials and low molecular weight. This explains why lithium can be considered more or less the perfect choice for the negative electrode: the combination of one of the lowest electrode potentials, $E^\circ = -3.05$ V, a high theoretical capacity of 3860 mAh/g and the lowest atomic weight of any solid material means that it has the best theoretical specific energy of all negative electrode materials [9]. The low density of lithium means that the theoretical energy density is lower than for some other systems, but it is still very good.

Lithium, combined with various positive electrodes, started to be commercialized in primary batteries during the 1970s but they were confined to niche applications due to high cost and problems with safety and reliability [9]. Progress with secondary batteries based on lithium was even slower until research began to focus on using intercalation compounds in the electrodes. These are materials with a layered structure that do not follow the ordinary reaction path when interacting with lithium but instead intercalate the atoms or ions, i.e. bind them weakly in between layers in the structure. The first commercial secondary lithium battery based on intercalation was introduced in 1991 by Sony and started the development that lead to the high performance Li-ion cells of today [8, 9].

The most common Li-ion rechargeable battery today uses a graphite negative anode that stores lithium, which on discharge is further oxidized to lithium cations Li^+ that travel through the electrolyte to the positive cathode where they are inserted into a lithium metal oxide, such as $LiCoO_2$ (LCO). The total reaction becomes

$$LiMO_2 + y\,C \underset{Charge}{\overset{Discharge}{\rightleftarrows}} Lix Cy + Li_{1-x}MO_2 \tag{2.2}$$

where M is a metal such as cobalt or manganese, $x \approx 0.5$ and $y = 6$ [1, 9, 10].

The cells use a nonaqueous electrolyte, which is required when using lithium due to its reactivity towards water. They have a voltage around 4 V, a wide temperature range and a flat discharge curve, a specific energy typically around 100 - 150 Wh/kg (up to 240 Wh/kg), an energy density up to 640 Wh/L and excellent cycleability. They are also free from memory effects, where the capacity of the cell depends on the DOD of previous cycles, that has been a large problem for some other secondary battery chemistries such as nickel-cadmium. Drawbacks are the high price and sensitivity to excessive charging and discharging - the chemistry does not have any built in limitations preventing damage when the operating range is exceeded. Li-ion batteries can also suffer from thermal runaway and even catch fire or explode. Newer batteries mitigate these problems through control electronics, better design and changed chemistry [9, 10].

The storage capacity of Li-ion batteries has roughly doubled since their introduction, enabling a firm grip on the high performance/high cost segment. The theoretical limit for the graphite and LCO chemistry is 387 Wh/kg and 1015 Wh/L, but current and future innovations are expected to be able to once again double todays already impressive performance. This work is mostly focused on improving the storage of lithium in the negative electrode, perhaps using spinels and/or tin alloys [9, 10].

2.1.2 Lithium sulfur batteries

Increasing the energy content by choosing different electrodes to further increase the voltage is difficult: even the combination of Li and F, found at the respective extreme ends of the E° range, would only produce a voltage of around 6 V. This would still only be a minor improvement over Li-ion batteries which already achieve > 4 V and may even reach more than 5 V with future improvements [2]. This route would also come with a huge increase in complexity because of the increasing reactivity of materials with higher electrode potentials.

Returning to equation (2.1) one can see that here is another way to improve the theoretical energy stored: by increasing n, the number of electrons exchanged in the reaction. This is a reason to study the reaction between lithium and sulfur which, during discharge, can be written as :

$$2\mathrm{Li} + \mathrm{S} \rightarrow \mathrm{Li_2S} \tag{2.3}$$

which can be split into the two half reactions:

$$\text{Negative electrode:} \qquad 2\mathrm{Li} \rightarrow 2\mathrm{Li^+} + 2\mathrm{e^-} \tag{2.4a}$$

$$\text{Positive electrode:} \qquad \mathrm{S} + 2\mathrm{e^-} \rightarrow \mathrm{S^{2-}} \tag{2.4b}$$

with the reactions being driven in the reverse direction during charge. Each sulfur atom will accept 2 electrons when fully reacted, immediately doubling the capacity compared to an element that only uses 1 electron. This, when combined with the low atomic mass of sulfur, is why the Li-S battery has the second highest theoretical specific energy of all Li battery chemistries at 2,567 Wh/kg, only beaten by the related lithium-air (Li-O_2) battery [1]. The low densities of lithium and sulfur means that, as previously seen when considering lithium alone, the energy density is not as exceptional, but it is still much better then current technology at 2,199 Wh/L [1]. Other large advantages are the abundance, low toxicity and environmental impact and very low cost of sulfur, implying that the batteries should have inherent low price compared to current technologies.

There are however several serious problems with Li-S batteries, as can be inferred from their lack of commercial success despite having been the subject of research since the 1940s. It is only in the last few years that real progress has been made and today there are some prototypes available, such as those made by Sion Power that deliver 350 Wh/kg with claimed near future improvement to around 600 Wh/kg [1]. One historic drawback is the low voltage, 2.2 V, especially compared to Li-ion [1]. This has become less of a concern as electronics has become smaller and more efficient meaning that higher voltages are only important for high power applications that already need large battery packs with multiple cells. The second most obvious problem is that both sulfur and the resulting lithium sulfide are insulating. The positive cathode must therefore contain a large fraction of

conductive additives such as carbon in addition to sulfur and care must be taken to minimize the buildup of Li_2S films during discharge.

The multiple electron reaction shown in (2.3) is deceptively simplified - sulfur naturally forms ring shaped molecules of 8 sulfur atoms, meaning that the reaction at least should be written as:

$$16Li + S_8 \rightarrow 8Li_2S \tag{2.5}$$

although this equation still manages to hide one of the largest sources of problems for Li-S cells: the polysulfides. The reduction of S_8 to S_8^{2-} goes through a whole zoo of intermediate polysulfide species S_n^{x-} with $2 \leq n \leq 8$. These reductions occur at different voltages and usually result in two reduction peaks in a cyclic voltammetry (CV) trace, instead of one peak as for simpler systems. The first peak is attributed to the reduction of S_8 to S_8^{2-} accompanied by four reactions involving the resultant species shown in (2.6) [11].

$$S_8 + 2e^- \rightarrow 2S_8^{2-} \tag{2.6a}$$
$$4S_8^{2-} \rightarrow 4S_6^{2-} + S_8 \tag{2.6b}$$
$$S_6^{2-} \rightarrow 2S_3^{\cdot -} \tag{2.6c}$$
$$2S_8^{2-} \rightarrow 2S_4^{2-} + S_8 \tag{2.6d}$$
$$S_8^{2-} + S_6^{2-} \rightarrow 2S_3^{2-} + S_8 \tag{2.6e}$$

For the second reduction peak the reactions in (2.7) have been suggested, as well as further reactions resulting in S_2^{2-}, S^{2-}, S_7^{2-} and S_5^{2-} [11].

$$S_8^{2-} + 2e^- \rightarrow S_8^{4-} \tag{2.7a}$$
$$S_8^{4-} \rightarrow 2S_4^{2-} \tag{2.7b}$$
$$S_6^{2-} + 2e^- \rightarrow 2S_3^{2-} \tag{2.7c}$$
$$S_3^{\cdot -} + e^- \rightarrow 2S_3^{2-} \tag{2.7d}$$
$$2S_3^{2-} + S_6^{2-} \rightarrow 3S_4^{2-} \tag{2.7e}$$
$$3S_8^{4-} \rightarrow 2S_6^{2-} + 4S_3^{2-} \tag{2.7f}$$

The nature of these reactions changes with solvent, electrolyte salt and electrode materials. Even for the same system the equilibria depend on temperature and concentration as well as the potential of the cell. There is still much debate on the exact behavior of the polysulfides, but there is no question about their importance.

The polysufides are generally capable of dissolving into the electrolyte, with the longer chained polysufides displaying better solubility, and will diffuse away from the positive electrode. They can then be reduced further to insoluble Li_2S_2 or Li_2S at other locations in the battery, forming deposits that increase the resistance and represent material loss. This is especially damaging when it occurs at the Li-metal electrode. The diffusing polysulfides cause current leakage and are involved in parasitic "shuttle" reactions where they are repeatedly shuttling back and forth between being reduced at the negative electrode and then oxidized at the positive electrode. This greatly accelerates the material loss and leads to lifetimes of at most a few cycles.

There are two main approaches to limit the problems caused by the polysulfides. The first is to use various microstructured cathode materials like mesoporous carbon that inhibit the diffusion of the polysulfides so that most are confined to the positive electrode until they have been sufficiently reduced [2, 12, 13]. This has improved the cycleability considerably, the price being added complexity. The other approach is to limit the dissolution and/or diffusion of polysulfides in the electrolyte by changing the solvent, using additives or even switching to a solid electrolyte [7, 14]. These approaches can in many cases be combined [5].

2.1.3 Ionic liquid electrolytes

The role of the electrolyte is to enable the exchange of ions between the electrodes of the cell while keeping them otherwise separated. It consists of a solvent, which can be aqueous, organic or inorganic, liquid or solid, and a salt providing mobile ions. It is even possible to have different electrolytes, separated by a membrane that is permeable to the ions only, in different parts of the battery [9]. The choice of electrolyte can have a large impact on the performance and one needs to take many different factors into account.

The components of the electrolyte should be chemically compatible with the other materials in the battery for the whole potential range, which can be determined through a simple CV measurement - a lack of reactions gives a flat curve without peaks. This means that it would not be possible to use an aqueous electrolyte in a battery containing lithium even if the lithium did not spontaneously react with water. The potential window of water is about 1.2 V which, being less than the voltage of most lithium batteries, would lead to the water being electrolyzed [9]. That the electrolyte is compatible does not necessarily require that it is totally passive with regard to the electrode materials. This is the case for many batteries using metallic lithium as the negative electrode where a solid electrode interface, SEI, will form on the surface. This is usually desirable, even though it lowers the conductivity, because it helps combat dendrite growth. When Li^+ ions are deposited on metallic lithium they tend to form dendrites which leads to loss

of active material and short circuits.

High ion conductivity is of course desirable, but many other physical properties are also important when constructing the battery. Good stability and a wide temperature range, low vapor pressure, non-flammability and nontoxicity will result in a battery with better performance and higher safety [9]. Most of the problems that have been reported with Li-ion batteries are caused by the organic electrolytes suffering thermal runaway: they start to decompose at elevated temperatures, increasing the resistance of the cell leading to further heating and so on. This led to battery packs catching fire and sometimes, when combined with poorly designed casing, even explosions.

One large class of solvents that has been receiving increased attention for use in battery electrolytes are ionic liquids (ILs). An ionic liquid is a salt that has a melting point below the operating temperature of the application. Room temperature ionic liquids (RTILs) are thus liquid at room temperature, with some remaining liquid far below the freezing point of water, making them particularly interesting for applications. All ionic liquids in this work are RTILs, and the terms will from now on be used interchangeably.

Ionic liquids generally have a high ion conductivity, high electrochemical and thermal stability, a wide liquid temperature range, large potential windows and very low vapor pressure. This provides potentially increased safety compared to current organic electrolytes, however the main reason for applying them to Li-S batteries is the hope that lower solubility of the polysulfides will solve some of the problems [7, 15].

An electrolyte could in theory consist of an IL alone, if it contained the correct ions. However the extremely low melting temperature compared with more standard salts like NaCl ($\sim 800\,^{\circ}\mathrm{C}$) is due to using large and asymmetric cat- and anions. The structures of the PP14-TFSI pair, one of four ILs used in this thesis, are shown in figure 2.2 as an example. This means that the active ions, Li^+ in the case of lithium batteries, still have to be added as an extra salt. A convenient way to minimize the number of ion species is to use the salt combining lithium with the anion in the IL resulting in a mixture of two cations and one anion.

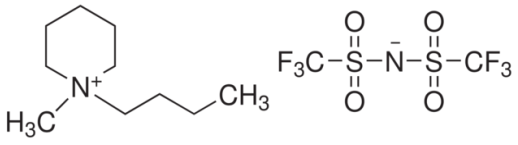


Figure 2.2: The structure of the PP14 cation (left) and the TFSI anion (right).

2.2 Characterizing batteries

A large amount of very useful information about the operation of a battery can be gained by relatively simple means due to the way they work: the most relevant facts are often the voltage, current and resistance, and how they change with time. These quantities are easy to measure with high precision and resolution with automated acquisition and even analysis by a computer. One of the most basic measurements is the discharge curve shown in figure 2.3 where the voltage as a function of time has been measured. The testing equipment ensures that a constant current flows during the discharge so that the x-axis is easily changed from time to capacity.

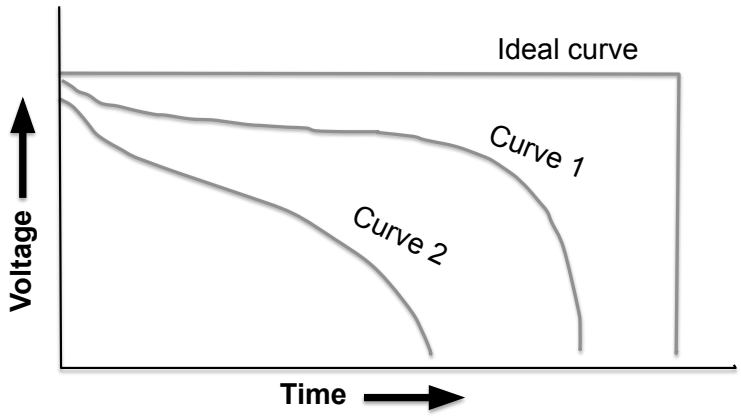


Figure 2.3: Cell voltage as a function of time (capacity) during discharge, showing both the ideal case and a general representation of a real battery.

For an ideal battery the discharge curve would show a constant potential equal to the OCV until the total capacity has been depleted and the voltage drops to zero. A real battery may start at OCV but will then show a sloping behavior, Curve 1 in figure 2.3, due to polarization and increasing internal resistance. The relatively flat section of the curve is called the plateau and defines the nominal voltage and is usually the voltage given for a battery, i.e. 1.5 V for alkali batteries. There may be multiple plateaus at consecutively lower voltages if there are several different reactions occurring during discharge. If the discharge current is higher (larger load) the resistive voltage drop and losses increase giving a lower and more sloped curve (Curve 2). The discharge is stopped at the cutoff voltage which is set as the point where most of the useful capacity has been used (primary batteries) or beyond which the battery would suffer loss of reversibility and/or damage (secondary batteries) [9].

The corresponding charge curve will show a similar, but reversed, behavior. The voltage during charging is always higher then during discharge and the hysteresis, due to losses, demonstrates the efficiency of the process. Multiple charge/discharge cycles are done in order to determine the cycleability or lifetime of the cell, with the end normally defined as a capacity of 80% of original capacity. In order to be commercially viable a battery is considered to need to withstand at least 300 cycles [8].

Chapter 3

Materials & Procedures

All materials and samples were handled in a glove box with a protective argon atmosphere in order to avoid contamination with water or oxygen. Samples containing sulfur species were stored wrapped in aluminum foil since some of them might be photosensitive [16]. When samples were removed for testing the vials and cuvettes were further sealed using Parafilm® M.

3.1 Ionic liquids

The following IL were used in the work presented in this thesis:

PP14-TFSI: 1-butyl-1-methylpiperidinium bis(triflouromethylsulfonyl)imide

PYR14-TFSI: 1-butyl-1-methylpyrrolidinium bis(triflouromethylsulfonyl)imide

BMIM-TFSI: 1-butyl-3-methylimidazolium bis(triflouromethylsulfonyl)imide

BMIM-SCN: 1-butyl-3-methylimidazolium thiocyanate

The first two were obtained from Sigma-Aldrich and the two imidazolium based ones from IOLITEC. Some of their basic properties can be seen in table 3.1 with the data provided by the suppliers.

These are all clear liquids at room temperature with PP14-TFSI being slightly yellow and BMIM-SCN having a strong yellow color. All electrolytes were made using lithium bis(triflouromethylsulfonyl)imide salt (LiTFSI), 99.95%, from Sigma-Aldrich in a 0.9:0.1 molar fraction. The electrolytes were stirred at 400 rpm and 60 °C for at least 12 h using a magnetic stirrer with a hot plate and temperature control. This was done to ensure homogeneity and complete dissolution of the salt. They were then stored at room temperature and stirred again before use.

Table 3.1: Properties of the ionic liquids.

IL	Formula	MW (g/mol)	ρ (g/cm^3)	Purity
PP14-TFSI	$C_{12}H_{22}F_6N_2O_4S_2$	436.43	1.34	97%
PYR14-TFSI	$C_{11}H_{20}F_6N_2O_4S_2$	422.41	1.40	98.5%
BMIM-TFSI	$C_{10}H_{15}F_6N_3O_4S_2$	419.36	1.43	99%
BMIM-SCN	$C_9H_{15}N_3S$	197.30	1.07	98%

3.2 Reference sample preparation

The reference samples were prepared using reagent grade sulfur powder and lithium sulfide powder (99%), both from Sigma-Aldrich, in stoichiometric proportions corresponding to Li_2S_4, Li_2S_6 and Li_2S_8 as well as pure S and pure Li_2S. The amount of powder was chosen so that the ratio of polysulfide to ionic liquid was 0.02 mol/mol (which corresponds to an molar fraction of ~ 0.0177). This concentration was based on the accuracy of the analytic balance used (± 0.1 mg) and the wish to minimize the amount of expensive IL. The powders were measured in a plastic weighing boat and then put in a vial with the corresponding amount of electrolyte and stirred at 400 rpm and 60 °C.

More dilute samples, with concentrations of 0.002, 0.001 and 0.0001 mol/mol (polysulfide/IL), were also prepared using the PP14-TFSI based electrolyte. These were made by first creating separate suspensions of S and Li_2S powders and then adding small amounts of the suspensions to a vial of electrolyte. These were then stirred and heated as before.

3.3 UV-Vis spectroscopy

The main experimental method used to investigate the polysulfide species present in the electrolytes was absorption spectroscopy with ultraviolet (UV) and visible light. This part of the electromagnetic spectrum has an energy that corresponds to electronic transitions of the valence electrons in atoms and molecules. In order for these electrons to interact with a photon its energy must closely match the energy difference between two of the electronic levels. This means that every element and compound will absorb or emit an unique set of wavelengths which therefore can be used as an "fingerprint" to identify the species present in a sample.

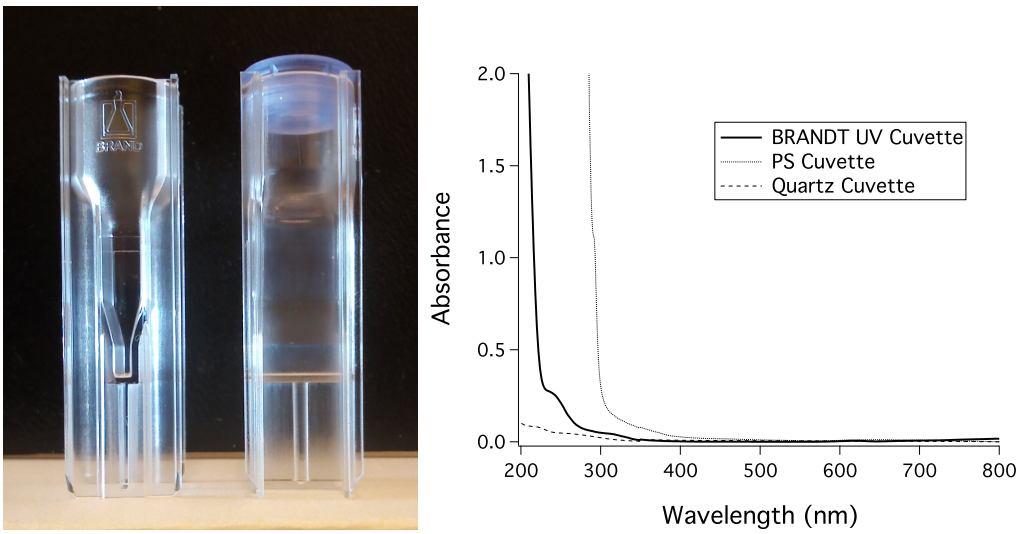
Absorption spectra are obtained by sending light of an known intensity through the sample and recording the resulting decrease in intensity as a function of wavelength. In the ideal case, a single element in a gaseous form, the spectra will consist of a collection of well-defined narrow lines. However, the chemical bonds

Table 3.2: Literature values for the wavelengths (in nm) of absorption peak maxima and their assigned polysulfide spices.

System	S_2^-	S_2^{2-}	S_3^{2-}	S_4^{2-}	S_5^{2-}	S_6^{2-}	S_7^{2-}	S_8^{2-}	S_3^-	S_4^-	Ref
DMF	250	280	344	420	435	340, 450	470	490 (S_{8l}^{2-}), 355 (S_{8c}^{2-})	600	∼700	[18]
[C_4mim][DCA]				440		∼350, 460			620		[11]

of molecules mean that their absorption wavelengths are changed by the presence of vibrational and rotational modes, turning single lines into collections of closely spaced lines which are themselves divided even further. The motion of the molecules combined with the limit of resolution of the instruments result in spectra with broad and often overlapping bands, especially in the case of liquid samples.

Absorption spectroscopy is a versatile, common, quick and easy to use method and has been used in much of the previous work on identifying polysulfides in solutions [11, 16, 17, 18, 19]. Many of the different peaks found in literature and their assigned species are shown in table 3.2.



(a) Front and side view with a cap.

(b) The absorbance of the BRAND™ UV cuvettes.

Figure 3.1: The BRAND™ UV cuvettes used for the UV-Vis absorption spectroscopy measurements.

The instrument used in this work is a Cary 5000 UV-Vis-NIR Spectrophotometer from Varian Inc. It uses a monochromator to select a specific wavelength from one of its broad-spectrum light sources, $175 - 3300$ nm. It has an exchangeable sample holder to enable many different kinds of samples and the light path is split to provide a reference beam if needed - this signal is subtracted from the

measurement.

The samples were put in disposable BRAND™ UV micro cuvettes (figure 3.1) which can hold samples of $70 - 550$ μL and have a path length of 10 mm. Plastic disposable cuvettes (usually made from PS or PMMA) are not transparent to UV light but these have a special composition that enable measurements from 220 to 900 nm, which is confirmed by a comparison of the spectra shown in figure 3.1b. Cuvettes made of quartz have superior optical properties and represent the ideal case, but they are orders of magnitude more expensive and require cleaning and reuse.

All spectra were taken using the default settings - a range from 800 down to 200 nm (with the data corresponding to the shortest wavelengths being discarded) and a scan speed of 3 nm/s using either air, an empty cuvette or an electrolyte sample as a reference.

3.4 Cyclic Voltametry

An other important tool was cyclic voltammetry, CV, the main electrochemical analysis method employed in this thesis. It can be seen as an inverse to the amperostatic discharge measurement - the voltage between the two electrodes is closely controlled and scanned at a constant rate while the resulting current is measured. The experimental setup for CV measurements uses three electrodes: the working electrode is the one being investigated, the counter electrode provides the current and the reference electrode is the reference point for the voltage. The counter electrode and the reference electrode can be the same physical electrode if the material is a convenient reference and has a good interface with the electrolyte.

The current produced depends on the charge transfer reactions that occur at the electrode. If no reactions are taking place at a certain voltage the corresponding current is only due to capacitive effects an can be neglected for low scan rates ($\sim$1 mV/s). The current will start to increase when the potential approaches that of the reaction, rapidly reaching a peak limited by the diffusion of the active species in the electrolyte. As these are depleted the current will decrease. When the potential sweep changes direction the reaction reverses and produces a second peak, see figure 3.2a. The current direction is defined so that the reduction peak is negative and the corresponding oxidation peak is positive. For instantaneous reactions with unlimited diffusion the result would be two sharp peaks at the same voltage, but even a very fast and highly reversible reaction will have a small potential difference between the two peaks (figure 3.2b). For systems with slow kinetics the peaks will be quite separated and broad, figure 3.2c, while an irreversible reaction only shows one peak as in figure 3.2d [9].

A single CV trace is an easy way to determine the voltages at which the dif-

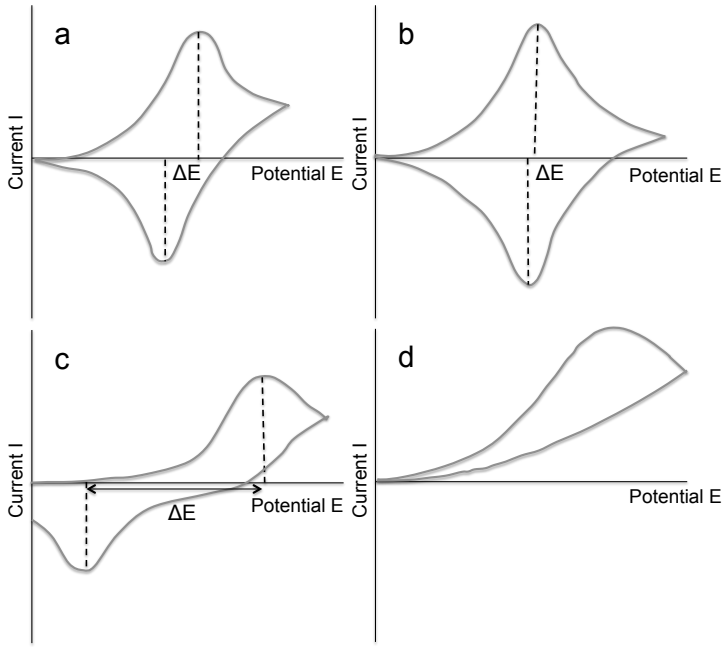


Figure 3.2: a) shows a generalized cyclic voltammogram for a reversible reaction with one reduction peak and one oxidation peak; b) is a very reversible system like a thin film deposited on the electrode while c) shows a quasi-reversible reaction. The result of an irreversible reaction is displayed in d).

ferent reactions in the cell occur, their reversibility and kinetics as well as whether there are several different reactions involved. More advanced measurements can provide further details by varying the scan speed and range and using different electrode materials and configurations.

3.5 Cell assembly and CV testing

The CV testing was performed using computer controlled Ivium-n-Stat battery tester with 8 channels. It can do both potentiostatic and galvanostatic measurements as well as frequency impedance analysis. For the CV traces the potential was set to the OCV of the cell and then scanned with 0.1 $\mathrm{mV/s}$ between 1.5 V and 3.2 V and the resulting current was measured.

The performance of the Li-S system with 0.9 PP14-TFSI + 0.1 LiTFSI electrolyte was tested using reusable Swagelok type cells. The design of these stainless steel cells is shown in figures 3.3 and 3.4: the bottom electrode is a cylinder with a round opening into which the piston shaped top electrode fits snuggly us-

ing an insulating Teflon ring. The top electrode is put in mechanical and electrical contact with the top cylinder through the use of a spring and the two cylinders are then firmly held together by the threaded fittings while being electrically insulated by more Teflon spacers. The very top and bottom of the cell have adjustable screws that can be connected to the battery tester.



Figure 3.3: The electrodes in a Swagelok cell, left to right is top to bottom.

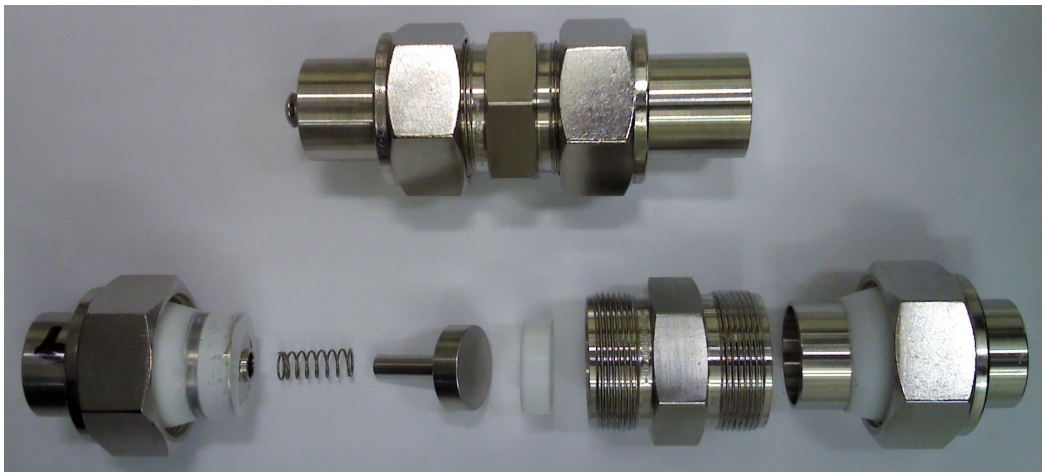


Figure 3.4: A complete Swagelok cell, assembled (top) and disassembled (bottom).

The active components of the cells were assembled in the following manner: the anode was cut from a 0.2 mm thick battery grade lithium metal foil using a 10 mm⌀ hole punch and put in the center of the bottom electrode after being pressed flat (Li is a very soft metal and is easily bent or deformed during handling). 8 µL of electrolyte were then put on top of the anode using a mechanical pipette together with a 14 mm⌀ separator membrane from Celgard® (type 2400: medium porosity 25 µm monolayer PP), followed by a 10 mm⌀ sulfur cathode. The cathode consist of a mixture of 60% S as the active material, 20% MWNTs to increase conductivity and 20% PVDF binder coated on an Al foil current collector.

The top electrode was then used to gently compress the anode-separator-cathode stack and the rest of the cell assembled. The spring ensured that there is a light compression providing good electrical contact and the Teflon seals makes the cell airtight so that it can be removed from the glove box and tested.

After testing the cell was disassembled and the separator, containing the majority of the electrolyte and the polysulfides of interest, was removed and put into a vial. 700 mg of electrolyte, approximately corresponding to a full cuvette, was then added to the vial and stirred together with the separator for 30 min @ 400 rpm. A sample was then extracted using a glass pipette, put into a cuvette and measured in the spectrophotometer.

Chapter 4

Results & Discussion

4.1 Reference samples

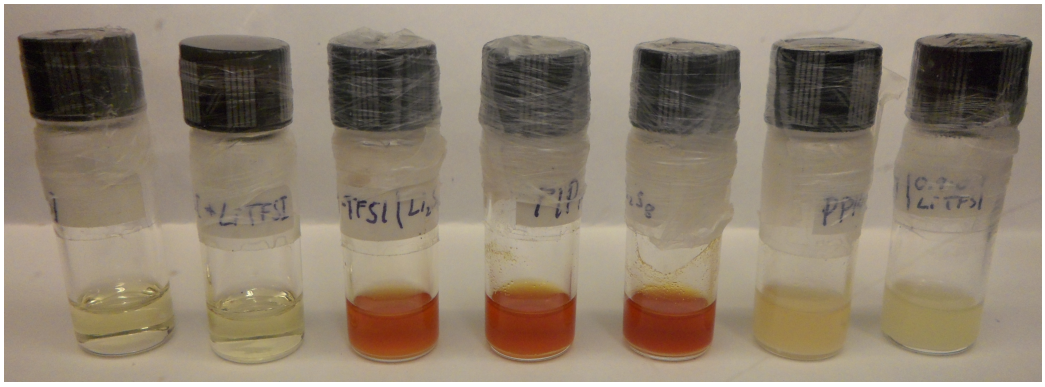


Figure 4.1: The reference samples made using PP14-TFSI electrolyte.
From left to right: pure IL, electrolyte and electrolyte containing Li_2S_4, Li_2S_6, Li_2S_8, S and Li_2S respectively.

Figures 4.1 to 4.4 show the reference samples that were the result of adding S and Li_2S to the electrolytes to obtain stoichiometric ratios corresponding to the polysulfides Li_2S_4, Li_2S_6, Li_2S_8 as well as S and Li_2S at a ratio of 0.02 mol per mol IL. Some results are quite clear and one can begin by looking at the two leftmost samples in each series. The addition of salt increased the viscosity of the electrolyte compared to the pure IL but did not alter the visual appearance for any of the ILs. Looking at the two rightmost samples it is apparent this also seems to be true for S and Li_2S - they form slowly precipitating suspensions that take on the combined color of the electrolyte and the powder but do not change the electrolyte

in any obvious way. The amount of precipitate implies that only a minor part of the already small amount of S or Li_2S actually dissolves in the electrolyte.

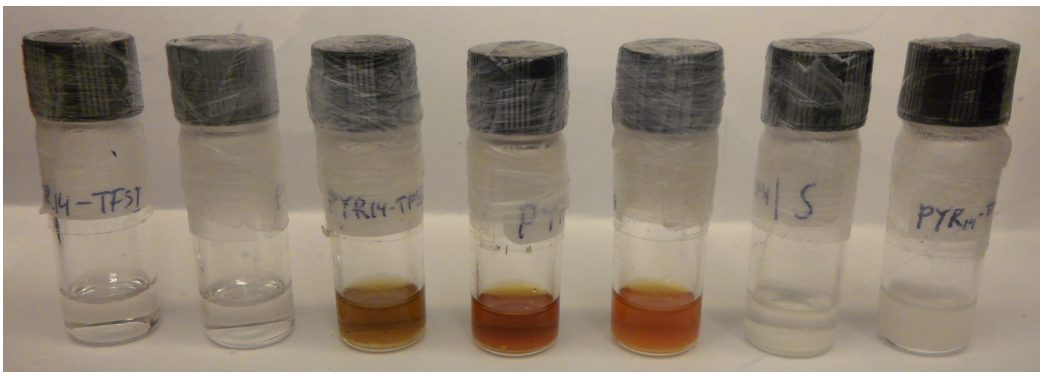


Figure 4.2: The reference samples made using PYR14-TFSI electrolyte. Left to right: pure IL, electrolyte and electrolyte containing Li_2S_4, Li_2S_6, Li_2S_8, S and Li_2S respectively.

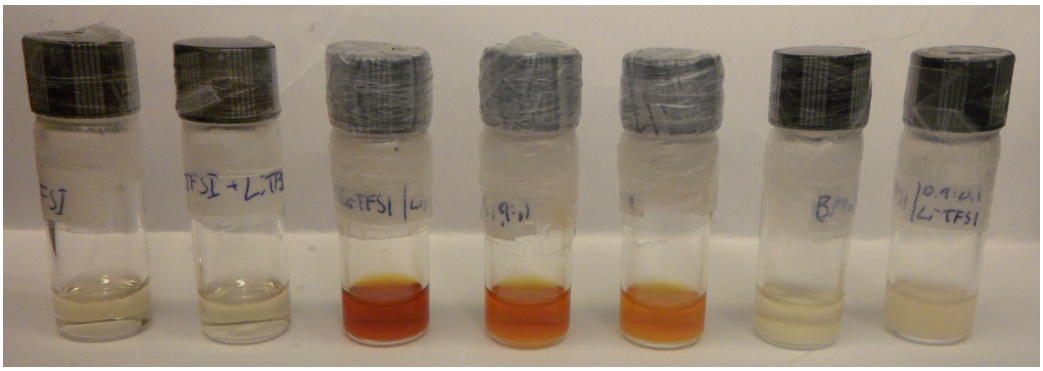


Figure 4.3: The reference samples made using BMIM-TFSI electrolyte.
From left to right: pure IL, electrolyte and electrolyte containing Li_2S_4, Li_2S_6, Li_2S_8, S and Li_2S respectively.

The color changes observed for the three "polysulfide" samples in all four cases are therefore a clear indication that a reaction has occurred and resulted in species that are soluble in the electrolyte. They are also quite stable, as demonstrated by the fact that the samples were first heated and then stored for an extended period of time without loosing their color. The relatively large amount of precipitate present in all of the samples does however mean that little can be learned of their actual composition by simply looking at them, even though some

small differences between some of the samples using the same electrolyte can be seen.

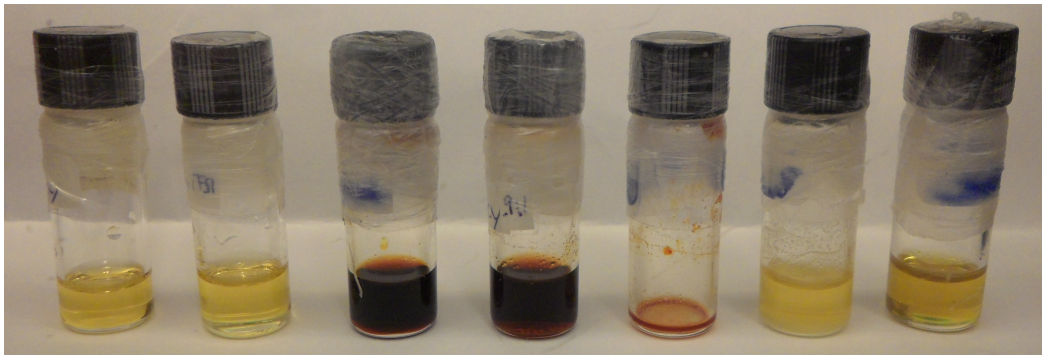


Figure 4.4: The reference samples made using BMIM-SCN electrolyte.
From left to right: pure IL, electrolyte and electrolyte containing Li_2S_4, Li_2S_6, Li_2S_8, S and Li_2S respectively. The Li_2S_8 sample, identical in appearance to the other two, was being tested.

4.1.1 Raman spectroscopy

It was originally planned that Raman spectroscopy would be one of the major techniques used. Raman scattering occurs when a photon scatters inelastically of an electron and interacts with a vibrational or rotational mode. It is therefore very sensitive to the finer details of bonds between atoms and molecules and their surroundings. This combined with the extensive experience of Raman spectroscopy in the group made it a logical starting point. There are also many examples of using Raman spectroscopy to investigate polysulfides in solution in the literature.

The method focuses monochromatic light from a laser on the sample and detect the very small shifts in wavelength that are the result of the interaction. The resulting spectra is often plotted as intensity as a function of the difference in inverse wavelength, which is proportional to the k-vector and measured in $/\text{cm}$, of the scattered light compared to the original laser wavelength.

One of the drawbacks of Raman spectroscopy is that the probability of a photon scattering inelasticity is low which results in a low signal to noise ratio. This combined with the low concentration of polysulfides in the samples resulted in spectra that were almost indistinguishable to those of the IL electrolyte. The lack of usable results, as demonstrated by figure 4.5, led to the decision to change method and use UV-Vis spectroscopy instead.

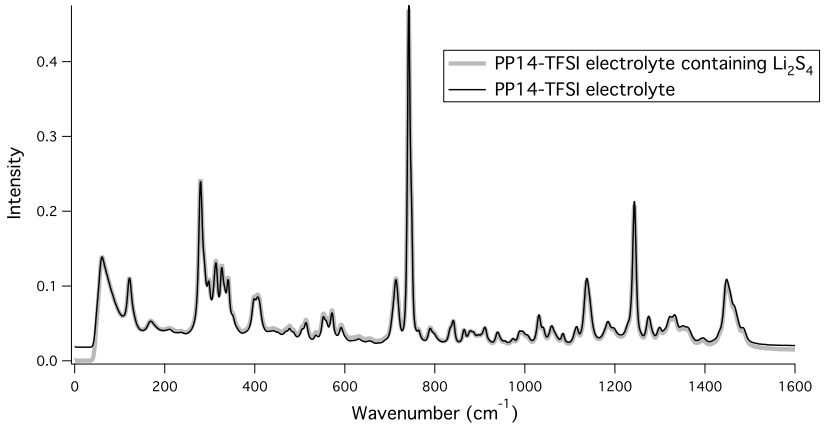


Figure 4.5: Raman spectra of the PP14-TFSI electrolyte with and without Li_2S_4.

4.1.2 UV-Vis spectroscopy

UV-Vis spectroscopy is capable of detecting very small concentrations of absorbing species. In this work the use of cuvettes with the standard 1 cm path length led to the opposite problem compared to Raman spectroscopy, i.e. too much signal, even though the Cary 5000 is capable of measuring up to an absorbance of 8. Only the pure PP14-TFSI and electrolyte samples produced useful spectra, shown in figure 4.6.

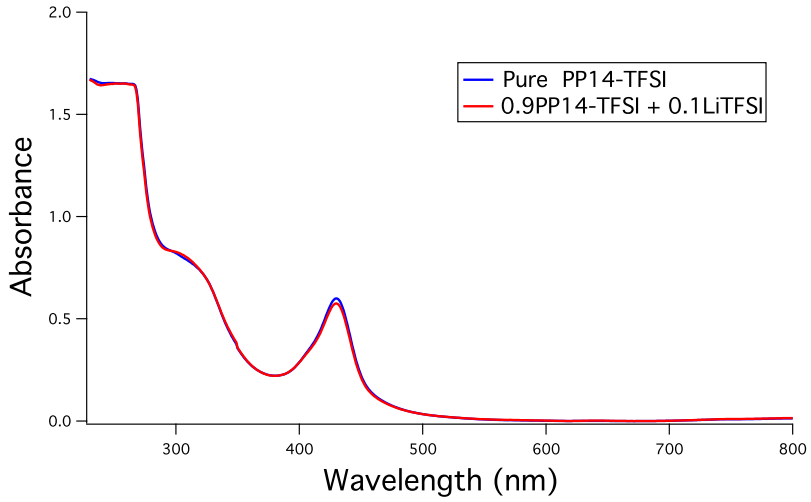


Figure 4.6: UV-Vis spectra of pure PP14-TFSI and 0.9 PP14-TFSI + 0.1 LiTFSI electrolyte.

The first thing to note is that the addition of LiTFSI salt does not affect the absorbance in the wavelength range covered. This was to be expected, since the salt and the IL share the TFSI anion and the electrolyte corresponds to exchanging 10% of the PP14 cations for Li^+ (which apparently does not have any discernible absorption lines in this range). The most important result, however, is that the electrolyte by itself does not absorb too strongly in the region of interest. It is therefore possible to use an electrolyte reference sample to compensate for the electrolyte signal and obtain the extra absorbance caused any polysulfides present.

The diluted reference samples were made in order to decrease the absorbance to a manageable level, which was found to require lowering the concentration from 20 mmol/mol (polysulfide/IL) to 0.1 mmol/mol. This concentration was low enough that there was very little or no visible color difference compared the electrolyte and that all powders dissolved completely. The lack of precipitate is also beneficial in two ways. It should improve the quality of the UV-Vis spectroscopy which is adversely affected by particles in the sample and it ensures that, although the composition of the resulting polysufides is uncertain, at least the amount of S and Li in the electrolyte are known. Figure 4.7 contains the resulting spectra.

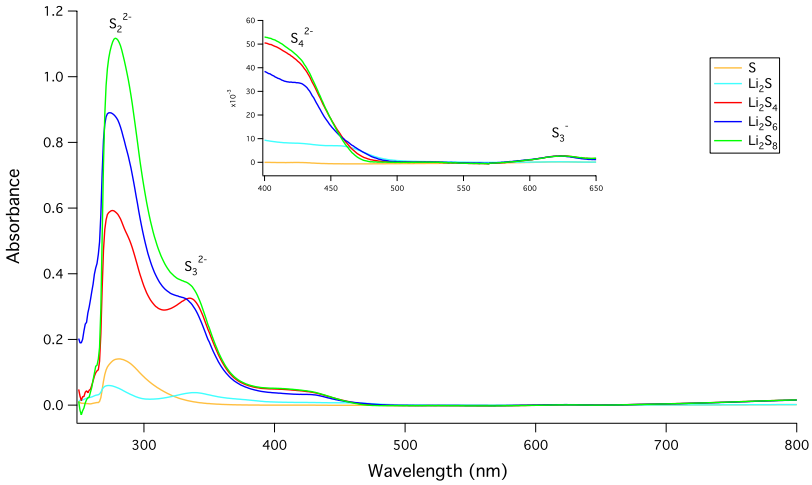


Figure 4.7: Spectra of the PP14-TFSI electrolyte containing S and Li_2S in the stoichiometric ratios of the polysulfides indicated. The insert is an enlargement of the 400-650 nm range.

Table 3.2, compiled from [11] and [18], was used to assign species to the peaks observed. The spectra for the three polysulfide samples are similar despite the different ratios of S and Li_2S, suggesting that the composition of the resulting polysulfides is mostly determined by their stability in the electrolyte. The peak

at 280 nm is due to S_2^{2-} according to [18] and is present in all samples, being the only clear peak in the pure S sample. The other three peaks easily identified in the spectra are two for S_3^{2-} and S_4^{2-} and a small one due to $S_3^{\cdot -}$. The intensity of the peaks for S_3^{2-} and S_4^{2-}, normalized by the signal for S_2^{2-}, are displayed in figure 4.8. It is clear from these two figures that higher ratios of Li to S results in a larger total amount of polysulfides, except when corresponding to the more stable Li_2S, and to more of the polysulfides being S_3^{2-} or S_4^{2-}.

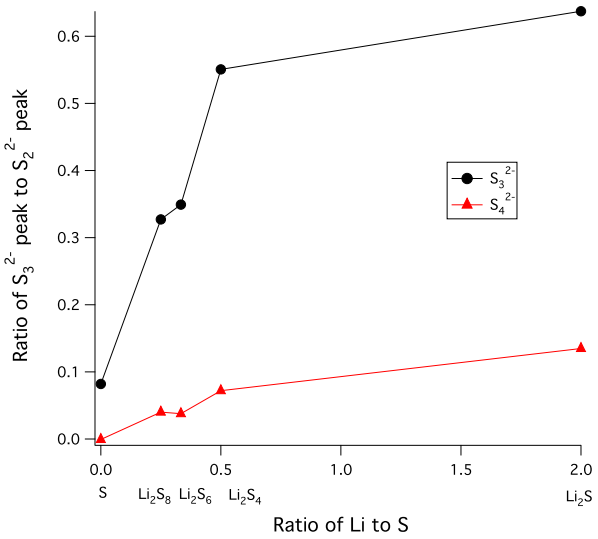


Figure 4.8: The height of the S_3^{2-} peak (black) and the S_4^{2-} peak (red) compared to the S_2^{2-} peak for the different ratios of lithium to sulfur.

The species present in these samples must result from the disproportion reactions of the polysulfides, as they were simply the result of mixing S and Li_2S - the two compounds containing sulfur and lithium that are stable outside of solutions. The weak absorbance for the radical $S_3^{\cdot -}$ is noteworthy: dilute solutions of S in some ILs produces enough of these species to turn the solution bright blue [19], while other ILs have been reported to strongly inhibit the formation of $S_3^{\cdot -}$ during discharge [11].

Multiple test of the same samples during one measurement session gave identical results, which demonstrates that the they are not degraded by the measurement itself. Redoing the measurements in figure 4.7 after storing the samples for 28 days gave the slightly different results shown in figure 4.9. These spectra imply that the S_3^{2-} is somewhat less stable in the PP14-TFSI electrolyte than S_4^{2-} and $S_3^{\cdot -}$.

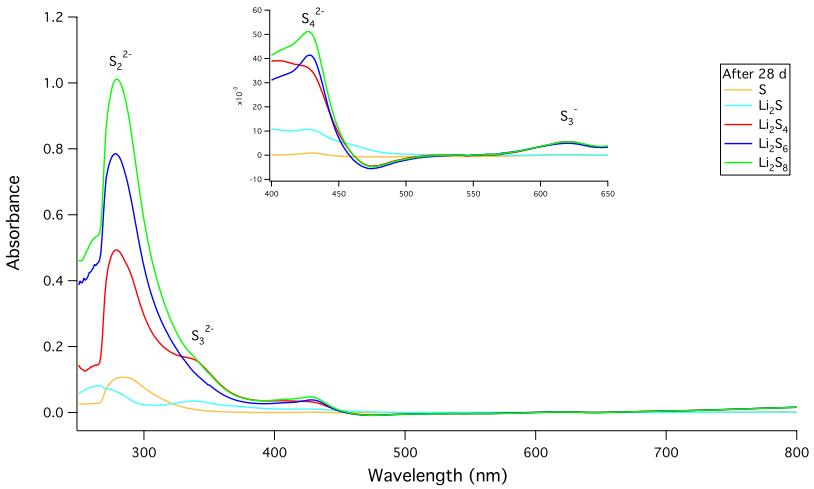


Figure 4.9: Spectra of the PP14-TFSI electrolyte containing S and Li_2S in the stoichiometric ratios of the polysulfides indicated, after 28 days of storage. The insert is an enlargement of the 400-650 nm range.

4.2 Tested cells

A number of cells were assembled and cycled to different points in the charge/discharge cycle in order to investigate the performance of the PP14-TFSI electrolyte in a Li-S battery and provide electrolyte samples for determining the polysulfide speciation. Figure 4.10 shows a 10 cycle test, the longest done in this work, that was stopped in the charged state at 3.2 V.

This trace shows a number of features, the first of which is the OCV at 3.03 V. Most cells tested had an OCV of either $\sim$ 3 V or $\sim$ 2.3 V. The reason for this is that the cell may self-discharge until it reaches the reduction peak. This requires very little actual current, as the flat CV trace shows, and may be initiated by a small imperfection or some disturbance during handling. Further self-discharge is much more limited: a cell stored for 130 days after assembly still showed an OCV of 2.34 V.

Instead of the two reduction peaks usually reported for Li-S cells during discharge [5, 11, 17] the trace in figure 4.10 has one broad peak. This is seen with IL based electrolytes [5, 7] because the slower kinetics, compared to organic electrolytes, widens the peaks and also displaces the peak voltage. The nonzero current at the end of the discharge shows that the reaction is still ongoing at this point. The same behavior, but with rapidly decreasing capacity, is seen during the following cycles.

The behavior during charge is similar but has some important differences. The

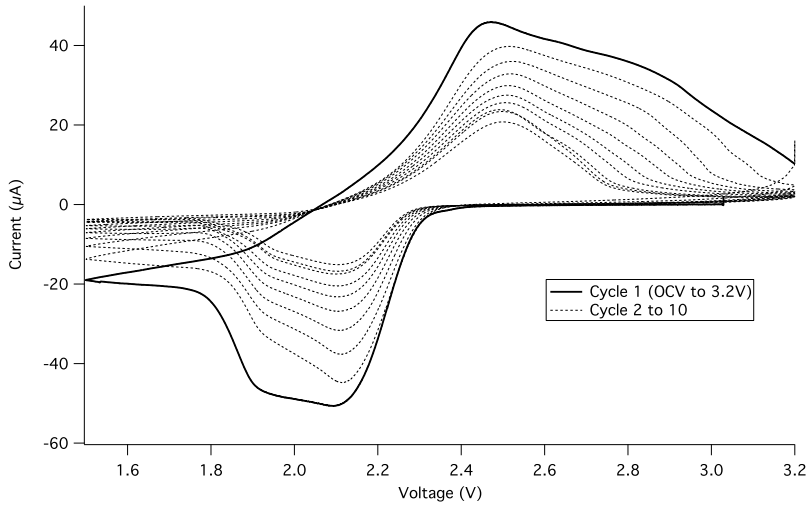


Figure 4.10: A typical CV trace over 10 cycles. The vertical line at 3.2 V is due to a slight pause in the measurement which allows charge to build up.

oxidation peak is a single peak with a large shoulder, demonstrating that the oxidation of the polysulfides continues throughout the charge with the easily oxidized species being consumed first and then progressively moving on to the long chain polysulfides. However, the shoulder rapidly disappears with continued cycling leading to the conclusion that these species are being lost, likely due to the formation of insoluble deposits.

Figure 4.10 suggests that there are five points during the cycle that should be of interests when doing UV-Vis spectroscopy to examine the polysulfide speciation. These are the first and the second part of the reduction peak at ~ 2.1 V and ~ 1.9 V, the discharged state at 1.5 V, the oxidation peak at ~ 2.4 V and finally the charged state at 3.2 V. The spectra corresponding to these points during the first charge/discharge cycle are shown in figure 4.11.

When analyzing these spectra it is important to remember that the absolute intensity of the peaks is dependent on the concentration of polysulfides. Even though the samples were all prepared in the same way there is no guarantee that the resulting concentrations are the same. The conclusions drawn can therefore only be based on the relative height of the peaks for each individual spectrum.

During the beginning of the reduction peak at 2.1 V during discharge the spectrum has a large contribution from S_6^{2-}, possibly combined with contributions from S_3^{2-} and S_7^{2-}. The concentration of S_3^{2-} increases and S_6^{2-} decreases toward the second part of the reduction peak at 1.9 V and when 1.5 V is reached there are large amounts of S_3^{2-} as well as S_4^{2-} with only a small amount of S_6^{2-} remain-

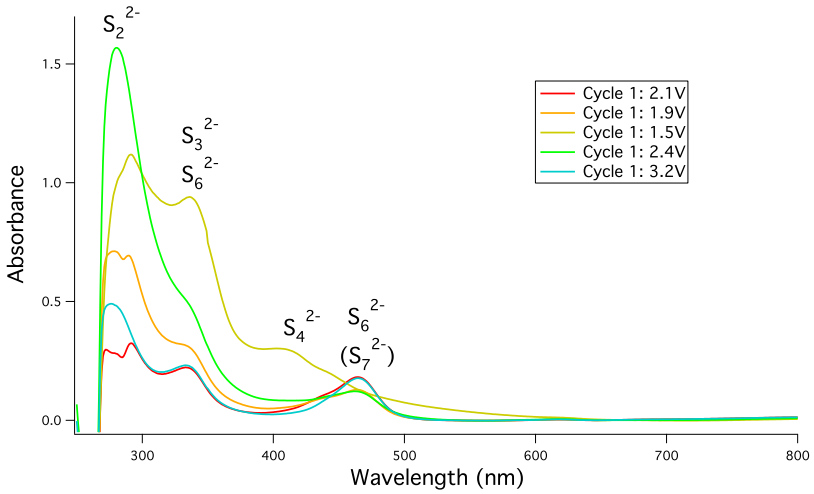


Figure 4.11: UV-Vis pectra taken from separators extracted from the first charge/discharge cycle at 2.1 V and 1.9 V during discharge, 1.5 V, 2.4 V during charge and 3.2 V.

ing. The process is then reversed during charging with S_4^{2-} rapidly decreasing followed by S_3^{2-} with S_6^{2-} increasing until the spectrum is almost identical to the original one.

These results agree with the results and reaction path suggested by the reference samples and reference [11], with S_6^{2-}, S_3^{2-} and S_4^{2-} as the main species involved. The exact location of the peaks and shoulders might suggest small contributions by longer chained polysulfides like S_7^{2-} and S_8^{2-} when the cell has been charged and by shorter polysulfides such as S_5^{2-}, created through the decomposition of S_3^{2-} as shown in (4.1) [18], when discharged.

$$2S_3^{2-} \rightarrow S_5^{2-} + S^{2-} \tag{4.1}$$

These species absorb at wavelengths close to those of the other polysulfides and would therefore be hard to detect in small amounts. The variations could also be due to the different solvent used as the values obtained have varied slightly in literature depending on the electrolyte system used.

Six more cells were assembled and tested in order to investigate the evolution of the polysulfides during cycling. These cells were stopped at the end of discharge (1.5 V) or the end of charge (3.2 V) during cycles 3, 6 and 10, producing the spectra shown in figures 4.12 and 4.13.

On the first cycle the cell further reduces most of the S_6^{2-} ions formed in the first part of the discharge to S_3^{2-} and S_4^{2-} as previously observed. The capacity

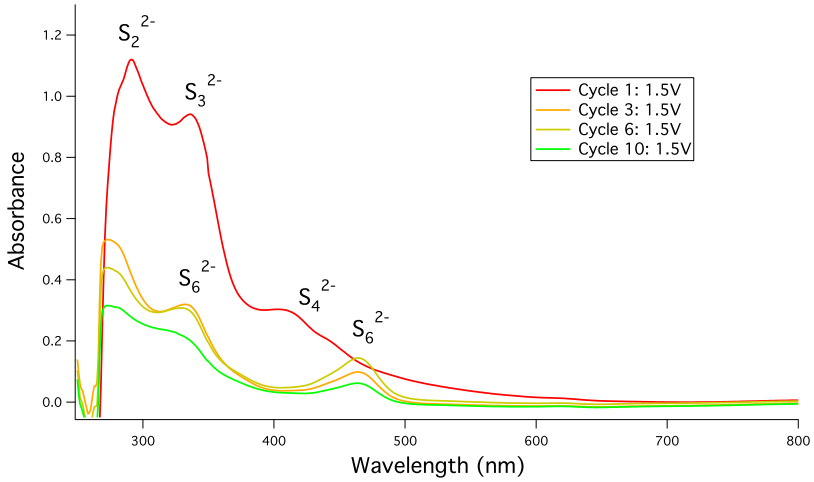


Figure 4.12: UV-Vis spectra taken from separators extracted at 1.5 V during cycles 1, 3, 6 and 10.

declines rapidly however and already by the third cycle there is a relatively large amount of S_6^{2-} left an no evidence of any S_4^{2-} , implying that only the first part of the reduction process occurs. The absorbance due to S_6^{2-} then becomes even weaker after more cycles as would be expected from the rapid decline in the current in the cyclic voltammogram (figure 4.10). The situation for the end of the charge, figure 4.13, follows the same pattern. While the first cycle involves the oxidation of most of the polysulfides present to at least S_6^{2-} the following cycles only show production of small amounts of S_6^{2-}, with most oxidation being only a few steps to short chained polysulfides.

As already mentioned the initial rate of self-discharge seen in these test cells varied widely even with careful assembly. None the less, all cells that were not tested immediately reached an OCV of ~ 2.3 V within a few hours and two cells that had been store for 24 h before being discharged showed much lower capacity indicating loss of active material. The final test was therefore done to record the absorption spectrum of the polysulfides present in a cell that had been allowed to self-discharge for an extended period of time, 130 days, resulting in figure 4.14.

The OCV of the cell before testing was 2.34 V suggesting that the reaction was still producing S_6^{2-} polysulfide ions. The spectrum contains the two S_6^{2-} peaks and a very weak S_2^{2-} peak, the weakest found for all tested samples. The total lack of other species demonstrates that the first reaction to occur in the Li-S battery using a PP14-TFSI electrolyte is the reduction of S_8 to S_8^{2-} through 2.6a which then rapidly dissociates into S_6^{2-} and S_8 according to 2.6b. If the S_6^{2-} ions diffuse to the

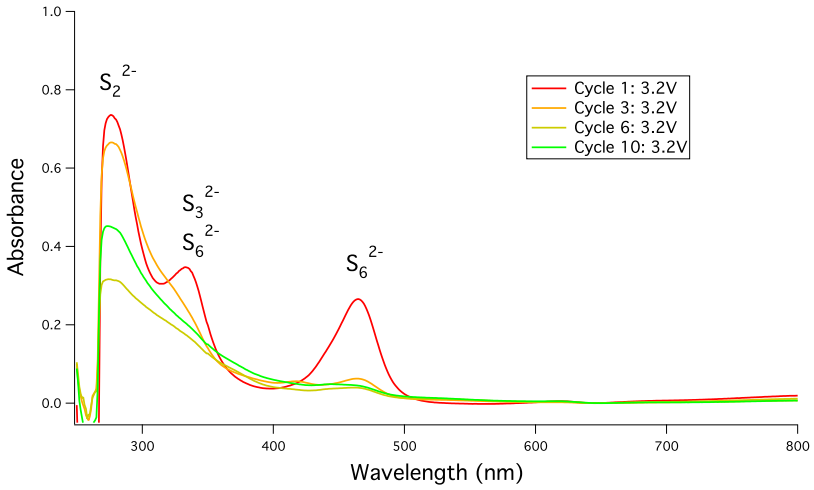


Figure 4.13: UV-Vis spectra taken from separators extracted at 3.2 V during cycles 1, 3, 6 and 10.

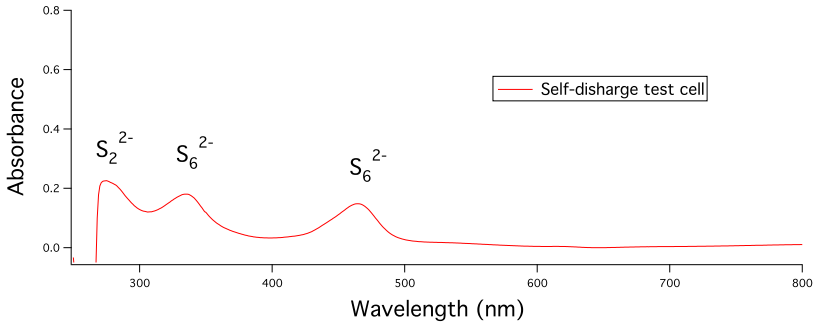


Figure 4.14: UV-Vis spectrum obtained by testing the separator from an assembled cell stored for 130 days to test the influence of self-discharge.

Li anode they will be further reduced and eventually lost, which would explain the rapid decline in capacity, however the low current behavior of the cell should only be determined by the production and mobility of the S_6^{2-} ions.

Chapter 5

Conclusion

The four RTIL investigated in this thesis, PP14-TFSI, PYR14-TFSI, BMIM-TFSI and BMIM-SCN, all made electrolytes that dissolved some polysulfide ions when S and Li_2S powders where added. This was evident due to strong changes in color when the electrolytes contained both S and Li_2S but not when mixed with either compound alone. The solubility, somewhat higher for BMIM-SCN compared to the other three ILs, was much lower than for most organic electrolytes and all but the lowest concentrations led to precipitation.

Deeper investigation of the 0.9 PP14-TFSI + 0.1 LiTFSI system using cyclic voltammetry, combined with absorption spectroscopy in the region $200 - 800$ nm on electrolyte samples taken from test cells, suggest the same reaction mechanisms in the IL electrolyte as found previously for organic electrolytes [11]. The IL electrolyte gives a CV trace that has one broad reduction peak instead of the two separate peaks observed for conventional electrolytes. The first reaction to occur during the discharge is the reduction of S_8 to S_6^{2-}, with the disassociation into S_3^- which often follows being strongly inhibited. The S_6^{2-} ions are then further reduced to S_3^{2-} and S_4^{2-} as the discharge proceeds. S_2^{2-} is present at all times but the reduction taking place in the electrolyte appears to be limited to S_3^{2-} and S_4^{2-}.

The reactions follow the opposite path during charging and shows good reversibility in that most of the shorter polysulfides are oxidized. There is however a large loss of the active species resulting in a rapidly declining capacity with cycling. This disagrees with [7] where it is claimed the lower solubility of polysulfides in PP14-TFSI electrolyte is enough to suppress the dissolution of the intermediate species and ensure good cycle ability. It should however be noted that the electrolyte used in that work had slightly more than three times the concentration of LiTFSI salt compared to the 0.9:0.1 molar ratio used for this thesis.

Chapter 6

Future Work

As is so often the case, the scope of this thesis had do be limited due to time constrains. However, research on this topic is still highly relevant and is continuing. Work has already been started/is being done i parallel/has been done in parallel to investigate the behavior of polysulfides in another ionic liquid using the methods developed here. This effort could be expanded even further to include the other ionic liquid electrolytes discussed earlier, other similar electrolyte systems of interest or differently structured sulfur cathodes.

Another possibility is to use an in situ cell to gain an even deeper understanding of the reactions during discharge and charge. Such work has been described in [17, 18] and enabled the continuous measuring of spectra for any point on the discharge/charge curve for the same cell. This setup could minimize many of the current sources of errors and might also enable measurements on the active surfaces themselves during cycling.

Bibliography

[1] P.G. Bruce, S.A. Freunberger, L.J. Hardwick, and J.M. Tarascon. Li–O2 and Li–S batteries with high energy storage. *Nature materials*, 11(1):19–29, 2011.

[2] Xue-Ping Gao and Han-Xi Yang. Multi-electron reaction materials for high energy density batteries. *Energy & Environmental Science*, 3(2):174, 2010.

[3] Xiulei Ji and Linda F. Nazar. Advances in Li–S batteries. *Journal of Materials Chemistry*, 20(44):9821, 2010.

[4] Bruno Scrosati, Jusef Hassoun, and Yang-Kook Sun. Lithium-ion batteries. A look into the future. *Energy & Environmental Science*, 4(9):3287, 2011.

[5] J Wang, S Y Chew, Z W Zhao, S Ashraf, D Wexler, J Chen, S H Ng, S L Chou, and H K Liu. Sulfur–mesoporous carbon composites in conjunction with a novel ionic liquid electrolyte for lithium rechargeable batteries. *Carbon*, 46(2):229–235, February 2008.

[6] M Galinski, A Lewandowski, and I Stepniak. Ionic liquids as electrolytes. *Electrochimica Acta*, 51(26):5567–5580, 2006.

[7] L.X. Yuan, J.K. Feng, X.P. Ai, Y.L. Cao, S.L. Chen, and H.X. Yang. Improved dischargeability and reversibility of sulfur cathode in a novel ionic liquid electrolyte. *Electrochemistry Communications*, 8(4):610–614, April 2006.

[8] Martin Winter and Ralph J Brodd. What are batteries, fuel cells, and supercapacitors? *Chemical reviews*, 104(10):4245–69, October 2004.

[9] Thomas B. Reddy and David Linden. *Linden's Handbook of Batteries, Fourth Edition.* McGraw-Hill, 4th ed. edition, 2011.

[10] Bruno Scrosati and Jürgen Garche. Lithium batteries: Status, prospects and future. *Journal of Power Sources*, 195(9):2419–2430, May 2010.

[11] Ninie S a Manan, Leigh Aldous, Yatimah Alias, Paul Murray, Lesley J Yellowlees, M Cristina Lagunas, and Christopher Hardacre. Electrochemistry of sulfur and polysulfides in ionic liquids. *The journal of physical chemistry. B*, 115(47):13873–9, December 2011.

[12] Guangyuan Zheng, Yuan Yang, Judy J Cha, Seung Sae Hong, and Yi Cui. Hollow carbon nanofiber-encapsulated sulfur cathodes for high specific capacity rechargeable lithium batteries. *Nano letters*, 11(10):4462–7, October 2011.

[13] Xiulei Ji, Kyu Tae Lee, and Linda F Nazar. A highly ordered nanostructured carbon-sulfur cathode for lithium – sulphur batteries. *Nature Materials*, 8(June), 2009.

[14] D Marmorstein, T H Yu, K A Striebel, F R Mclarnon, J Hou, and E J Cairns. Electrochemical performance of lithiumrsulfur cells with three different polymer electrolytes. *Journal of Power Sources*, pages 219–226, 2000.

[15] Joon Ho Shin and Elton J. Cairns. Characterization of N-Methyl-N-Butylpyrrolidinium Bis(trifluoromethanesulfonyl)imide-LiTFSI-Tetra(ethylene glycol) Dimethyl Ether Mixtures as a Li Metal Cell Electrolyte. *Journal of The Electrochemical Society*, 155(5):A368, 2008.

[16] P. Dubois, JP Lelieur, and G. Lepoutre. Chemical species in solutions of sulfur in liquid ammonia. *Inorganic Chemistry*, 26(12):1897–1902, 1987.

[17] Yajuan Li, Hui Zhan, Suqin Liu, Kelong Huang, and Yunhong Zhou. Electrochemical properties of the soluble reduction products in rechargeable Li/S battery. *Journal of Power Sources*, 195(9):2945–2949, May 2010.

[18] Dong-Hun Han, Bum-Soo Kim, Shin-Jung Choi, Yongju Jung, Juhyoun Kwak, and Su-Moon Park. Time-Resolved In Situ Spectroelectrochemical Study on Reduction of Sulfur in N,N'-Dimethylformamide. *Journal of The Electrochemical Society*, 151(9):E283, 2004.

[19] Eva Boros, Martyn J Earle, Manuela a Gîlea, Andreas Metlen, Anja-Verena Mudring, Franziska Rieger, Allan J Robertson, Kenneth R Seddon, Alina a Tomaszowska, Lev Trusov, and Joseph S Vyle. On the dissolution of non-metallic solid elements (sulfur, selenium, tellurium and phosphorus) in ionic liquids. *Chemical communications (Cambridge, England)*, 46(5):716–718, February 2010.